

# Journal of Materials Chemistry A

Accepted Manuscript



This is an *Accepted Manuscript*, which has been through the Royal Society of Chemistry peer review process and has been accepted for publication.

*Accepted Manuscripts* are published online shortly after acceptance, before technical editing, formatting and proof reading. Using this free service, authors can make their results available to the community, in citable form, before we publish the edited article. We will replace this *Accepted Manuscript* with the edited and formatted *Advance Article* as soon as it is available.

You can find more information about *Accepted Manuscripts* in the [Information for Authors](#).

Please note that technical editing may introduce minor changes to the text and/or graphics, which may alter content. The journal's standard [Terms & Conditions](#) and the [Ethical guidelines](#) still apply. In no event shall the Royal Society of Chemistry be held responsible for any errors or omissions in this *Accepted Manuscript* or any consequences arising from the use of any information it contains.

**Rapid Phosphine-Free Synthesis of CdSe Quantum Dots:  
Promoting the Generation of Se Precursors  
by a Radical Initiator**

Bo Hou,<sup>a</sup> David Benito-Alifonso,<sup>a</sup> Richard Webster,<sup>b</sup> David Cherns,<sup>b</sup>

M. Carmen Galan<sup>a</sup> and David J. Fermín<sup>a\*</sup>

<sup>a</sup> School of Chemistry, University of Bristol, Cantocks Close, Bristol BS8 1TS, UK

<sup>b</sup> School of Physics, University of Bristol, Tyndall Avenue, Bristol BS8 1TL, UK

\*To whom correspondence should be addressed.

E-mail: David.Fermin@bristol.ac.uk.

URL: <http://www.chm.bris.ac.uk/pt/electrochemistry> Tel.: +44 117 9288981.

## Abstract

The replacement of phosphine containing compounds in the synthesis of II-VI quantum dots (QDs) via the ‘hot-injection’ method has received considerable attention in recent years, in particular toward scaling-up production. A key bottleneck in current approaches is the poor solubility of elemental Se in solvents such as 1-octadecene (1-ODE) or oleylamine requiring heating temperatures of 200°C for several hours, or the introduction of additives such as alkylthiols or NaBH<sub>4</sub>, or replacement by SeO<sub>2</sub>. In the present work, we elucidate the fundamental steps in the dissolution of elemental Se in 1-ODE and oleylamine with the view of facilitating the large-scale synthesis of CdSe QDs. The main organoselenium species generated during the solubilisation of elemental Se in 1-ODE and oleylamine were identified by 1D and 2D NMR (<sup>1</sup>H, <sup>13</sup>C and <sup>77</sup>Se). Experimental evidences suggest that the rate determining step is the formation of Se radicals, via homolytic cleavage of Se-Se bond, that attack the allylic proton in 1-ODE and oleylamine. Plausible reaction pathways in both systems are proposed. Finally, we demonstrate that the radical-mediated solubilisation of Se can be significantly accelerated by the addition of azobisisobutyronitrile (AIBN), a common radical initiator used in the polymer industry. In this way, highly concentrated Se precursor was prepared. The “hot- injection” of the Se precursor, into CdO containing 1-ODE solution leads to the formation of highly luminescent CdSe QDs with well-defined cubic structure.

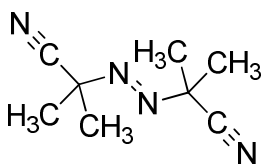
## 1. Introduction

The optical properties of CdSe quantum dots (QDs) have generated tremendous interest due to their potential exploitation in a variety of fields including light-emitting devices,<sup>1</sup> imaging probes<sup>2</sup> and absorber layers in photovoltaic devices.<sup>3</sup> Colloidal synthesis is widely recognized as key for large-scale fabrication of highly monodispersed and stable QDs. The seminal work by Murray et al.<sup>4</sup> introduced the methodology of injecting phosphine-chalcogenide precursors into an organometallic solution at temperatures above 300°C.<sup>4b</sup> Another important contribution in the field was made by Peng and co-workers, replacing the highly unstable organometallic precursors by metal oxide (e.g. CdO) in the presence of stearic acid.<sup>5</sup> With regards to the solubilization of the chalcogenide component, Lewis bases such as tributylphosphine (TBP) or trioctylphosphine (TOP) have been extensively used.<sup>6</sup> However, these phosphines are highly flammable and corrosive,<sup>7</sup> prompting the search for alternative approaches.

Mulvaney and co-workers reported the first phosphine-free synthesis of CdSe, based on the dissolution of Se in 1-octadecene (1-ODE) after prolonged periods of heating at high temperatures.<sup>8</sup> Subsequently, other research groups have employed similar approaches to synthesize phosphine-free nanocrystals.<sup>9</sup> Solvents such as olive oil,<sup>10</sup> paraffin,<sup>11</sup> and oleylamine<sup>12</sup> have also been implemented. In addition<sup>12</sup> to long time heating protocols aimed at facilitating the dissolution of Se, additives including NaBH<sub>4</sub><sup>13</sup> and alkylthiols<sup>14</sup> have been introduced. The disadvantage of the latter approaches is the introduction of additional elements (eg. Na, B, S) which could appear as impurities in the final product. Recent studies have demonstrated that the synthesis of QDs can be carried employing insolubilized Se<sup>15</sup> or SeO<sub>2</sub><sup>16</sup> powder with good yields. In these approaches, the reported Se concentration in precursor solution is not higher than 0.2 mol×dm<sup>-3</sup>, which represents a bottleneck towards scale-up. In order to make the reaction suitable to industrial scope, a good understanding of the Se dissolution process is crucial. Raston and co-workers proposed that Se-Se and Se-C bonding compounds are the main species after the dissolution of Se into 1-ODE.<sup>17</sup> However, the mechanism of formation and nature of the Se precursors in these solvents remain to be fully elucidated.

In this work, we investigate the process involved in the dissolution of Se in 1-ODE and oleylamine by NMR, FTIR and mass spectroscopy, with the aim of optimizing this key step which is considered the bottleneck in the phosphine-free synthesis of CdSe QDs.<sup>12b, 14</sup>

Our results confirm that the process is initiated by the attack of thermally generated Se radicals to the allylic position of 1-ODE upon heating at temperatures above 200°C, in agreement with previous studies.<sup>17</sup> We show that this reaction manifests itself by the migration of the terminal olefin group in 1-ODE and *cis/trans* isomerisation in oleylamine, generating a range of organoselenium structures. Furthermore, we show for the first time that Se dissolution in 1-ODE can be significantly accelerated by addition of trace amounts of the radical initiator azobisisobutyronitrile (AIBN, **I**). This approach not only allows the preparation of Se precursor solutions with concentrations as high as 1.0 mol×dm<sup>-3</sup>, but also the facile synthesis of highly luminescent CdSe QDs under phosphine-free condition yielding phase-pure monodispersed cubic nanocrystals.

**I**

## 2. Experiment

### 2.1. Se dissolution in 1-ODE and oleylamine

The dissolution of elemental Se (3mmol) into 1-ODE (9 mmol, 2.88 cm<sup>3</sup>) or oleylamine (9 mmol, 4.23 cm<sup>3</sup>) was investigated by taking aliquots of the reaction mixture during the following heating program: room temperature (step I), 60°C for 30min under vacuum (step II), 130°C for 30min under vacuum (step III), 200°C for 30min (step IV) and 20h (step V) under Ar. Each aliquot was analysed by 1D <sup>1</sup>H, <sup>13</sup>C and 2D NMR, as well as FTIR spectroscopy. The concentration of the final Se solution in 1-ODE or oleylamine is 1.04 and 0.71 mol×dm<sup>-3</sup>, respectively.

### 2.2. Facile Se dissolution promoted by AIBN

Following a similar procedure as in the previous experiment, a mixture of Se and 1-ODE (1.04 mol×dm<sup>-3</sup>) was prepared with the addition of 0.6 mg of AIBN at room temperature. The

composition of the solution was investigated at room temperature under Ar (step I) and after heating at 200°C for 1h (step II), 2h (step III) and 3h (step IV).

### 2.3. Phosphine-free synthesis of CdSe QDs

The QDs were prepared based on the method reported by Peng<sup>18</sup> with a commonly employed Se precursor concentration (0.1 mol×dm<sup>-3</sup>). Typically, Se (0.0395 g) and 1-ODE (5 cm<sup>3</sup>) are loaded into a 50 cm<sup>3</sup> two-neck flask and heated at 60°C under vacuum for 1h, followed by addition of 0.001 g of AIBN (1% mol/mol). The temperature is subsequently increased to 200°C for 1h under Ar, leading to the dissolution of Se (clear yellow solution). CdO (0.0254 g), stearic acid (0.228 g) and 1-ODE (20 cm<sup>3</sup>) were introduced into a 250ml three-neck round bottom flask and dried in vacuum at 100°C for 30 min. The metal-precursor solution was subsequently heated to 320°C under an Ar atmosphere. Once the solution became colourless, the Se precursor was quickly injected into the cadmium solution. The particles were allowed to grow for different times at 320°C, after which the heating mantle was removed. The QDs were purified by dissolving in a methanol:hexane mixture (v:v=3:1) and centrifuged for 10 min to remove the 1-ODE, followed by addition of acetone and further centrifugation. The precipitate was dissolved in chloroform for further characterization.

### 2.4. NMR, FTIR and electron microscopy methodologies and instrumentation

Reactions requiring anhydrous conditions were performed under an atmosphere of either anhydrous nitrogen or argon. All glassware was flame-dried prior to use and glass syringes and needles were placed in an oven (150°C) for at least 2h and allowed to cool in desiccators under an atmosphere of anhydrous nitrogen. Aliquots from the reaction mixture were collected at different stages of the heating programme under an Ar atmosphere and samples allowed to cool to room temperature before analysis. 1D, 2D <sup>1</sup>H NMR and <sup>13</sup>C NMR spectra such as 2D proton correlation spectroscopy (COSY), carbon-proton heteronuclear single quantum correlation (HSQC) and carbon-proton heteronuclear multiple-bond correlation spectroscopy (HMBC) were measured in a 400 MHz Varian INOVA 400 instrument. Chemical shifts are quoted in parts per million (ppm) and referenced to SiMe<sub>4</sub> (<sup>1</sup>H NMR 0 ppm) and CDCl<sub>3</sub> (<sup>13</sup>C NMR 77.16 ppm). The <sup>13</sup>C NMR sequence parameters were set up as follows: 45° pulse of 7.70 μs, τ<sub>2</sub> = 1.0 s, and acquisition time of 1.28 s. The 1D and 2D <sup>77</sup>Se NMR spectra including 1D proton decoupled <sup>77</sup>Se NMR and 2D proton-selenium HMBC, were measured in a 500MHz Varian INOVA 500 instrument. The <sup>77</sup>Se NMR sequence parameters were set up as follows: 45° pulse, τ<sub>2</sub> = 1.0 s, and acquisition time of 0.860 s. A saturated solution of diphenyldiselenide in CDCl<sub>3</sub> was used as an external standard.<sup>19</sup> FTIR

spectra were obtained using a Perkin-Elmer Spectrum 100 FTIR Spectrometer. The structure of the CdSe dots was investigated by powder XRD (BRUKER D8, Cu K $\alpha$  radiation  $\lambda = 1.54\text{\AA}$ ), JEOL 200 kV Hi Resolution TEM 2011 fitted with an EDX Oxford Instruments ISIS 300 system. Selected area electron diffraction (SAED) analysis was performed using a Phillips EM430 instrument with a camera length set at 270 mm and the electron wavelength at 0.251  $\text{\AA}$ .

### 2.5. Electrospray ionization (ESI) and negative ion matrix assisted laser desorption ionization time-of-flight (MALDI-TOF) mass spectrometry (MS) analysis of Se-containing product

In the 1-ODE system, the Se containing products were isolated by silica gel flash column chromatography using hexane as the eluent. In the oleylamine system, the Se containing products are isolated through vacuum distillation using a Kugelrohr apparatus. The isolated products were dried under vacuum and re-dissolved into dichloromethane for ESI<sup>+</sup> analysis. MALDI analyses were recorded using a HP MALDI instrument (Applied Biosystems 4700 Proteomics Analyzer) using gentisic acid as the matrix.

## 3. Results and Discussion

### 3.1. Analysis of the Se precursor in 1-ODE

Figure 1 displays NMR and FTIR spectra of the Se/1-ODE mixture at the various heating steps. <sup>13</sup>C NMR spectra show the emergence of new signals at  $\delta = 124.4$  and  $131.7$  ppm (Figure 1a) after heating at 200°C for 20 h under an Ar atmosphere (step V). <sup>1</sup>H NMR data also revealed the appearance of a new multiplet signal at  $\delta = 5.42$  ppm at step V (Figure 1b). The appearance of these signals occurs only after the complete dissolution of Se in 1-ODE. A comparison of the 2D HSQC NMR of the solutions in steps I (figure 1c) and V (figure 1d) reveals the appearance of *cis* and *trans* carbon-proton correlations in the latter step, suggesting the migration of the terminal olefin moiety to form 2-octadecene (2-ODE). This analysis is supported by 2D COSY NMR spectrum of sample V showing the olefinic protons ( $\delta=5.41$  and  $5.43$  ppm) are correlated with protons found at  $\delta = 1.63$  and  $1.94$  ppm (see supporting information [S3]), while the HSQC spectrum in Figure S4 indicates that the protons at  $\delta = 1.63$  and  $1.94$  ppm are bonded with carbons at  $\delta = 18.0$  and  $32.7$  ppm, which are attributed to CH<sub>2</sub> and CH<sub>3</sub> moieties. Furthermore, the decrease of the IR bands at  $\nu = 991$

and  $908\text{ cm}^{-1}$  and the emergence of a band at  $\nu = 964\text{ cm}^{-1}$  (figure 1e) are also consistent with the formation 2-ODE.

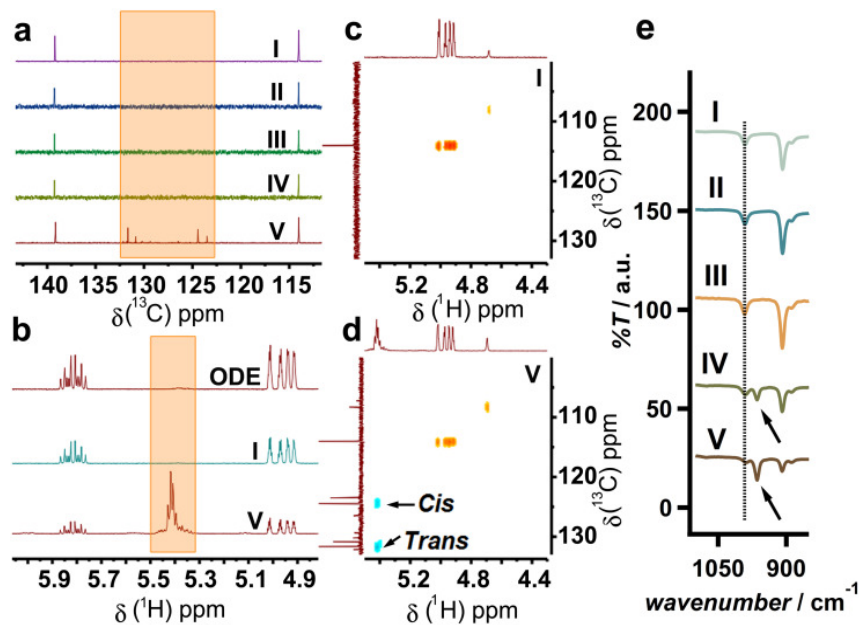
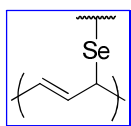


**Figure 1.**  $^{13}\text{C}$ -NMR analysis of Se in 1-ODE at room temperature (step I),  $60^\circ\text{C}$  for 30min under vacuum (step II),  $130^\circ\text{C}$  for 30min under vacuum (step III),  $200^\circ\text{C}$  for 30min (step IV) and 20h (step V) under Ar (a).  $^1\text{H}$ -NMR of the solution precursor in steps I and V, as well as of 1-ODE after heating at  $200^\circ\text{C}$  for 20h under Ar in the absence of Se (b). The highlighted areas in (a) and (b) correspond to the signal associated with the olefin functional group. HSQC 2D NMR of Se containing solutions in steps I (c) and step V (d). The arrows indicate the correlation between  $^{13}\text{C}$ - $^1\text{H}$  from *cis* and *trans* olefin moiety. FTIR analysis of the precursor solutions in steps I to V (e). The arrows indicate a vibrational mode associated with the olefin moiety in *trans* 2-octadecene, while the dotted line indicates the position of the equivalent vibrational model in 1-ODE.

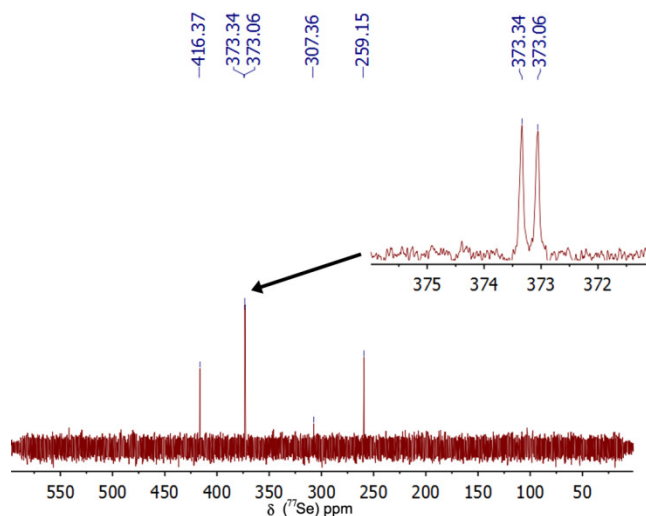
Figure 2 shows the  $^{77}\text{Se}$  NMR analysis of Se precursor at step V after purification by chromatography. The NMR signals with chemical shifts of 416.4 (singlet), 373.1 (singlet), 373.3 (singlet), 307.4 (singlet) and 259.2 ppm (singlet) are consistent with dialkyl polyselenides species.<sup>20</sup>  $^1\text{H}$ ,  $^{13}\text{C}$ , and  $^{77}\text{Se}$  1D and 2D NMR analysis (figure 3 and supporting information [S4]), confirmed the formation of a carbon-selenium bond during the solubilisation process. The species formed are a mixture of structural isomers with similar properties, complicating their isolation. A thorough study of the mixture shows, as a common feature, the presence of an olefinic group alpha to the C-Se bond.





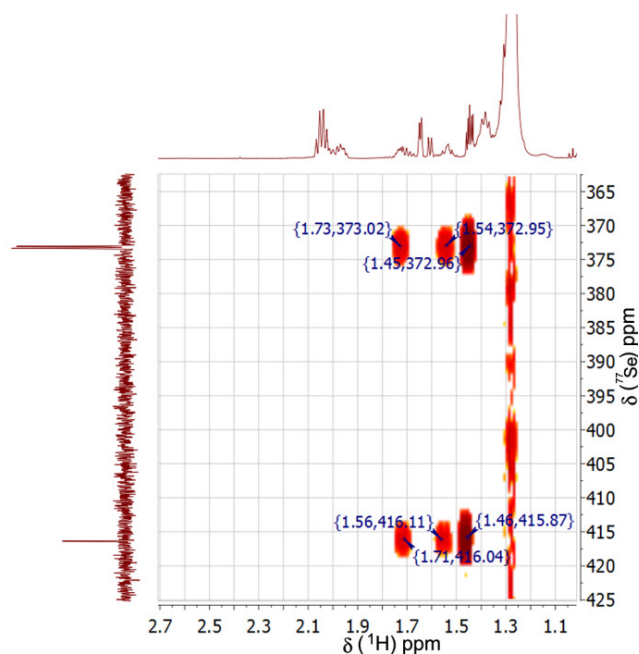
dialkyl polyselenides

## II



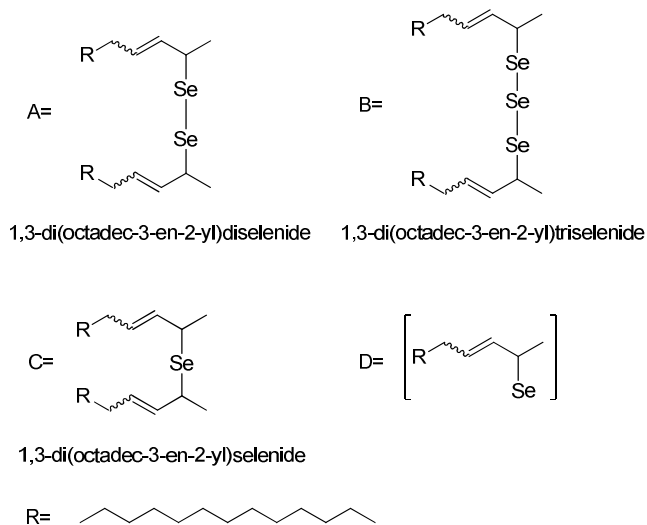
**Figure 2.** Proton decoupled  $^{77}\text{Se}$  NMR spectrum of the purified Se intermediate generated after dissolution 1-ODE after 20h at 200°C under Ar. Inset shows two closed peaks with chemical shifts of 373.3 and 373.1 ppm.

Figure 3 shows the 2D  $^1\text{H}$  and  $^{77}\text{Se}$  HMBC NMR spectra of Se containing species, confirming the Se bonding to a secondary carbon. The 2D  $^1\text{H}$  and  $^{13}\text{C}$  HMBC NMR spectra in figures S5 and S6 (see Supporting Information [S4]) suggest the secondary carbon bound to Se is next to an olefinic carbon and a saturated carbon. The 2D  $^1\text{H}$  and  $^{13}\text{C}$  HSQC NMR spectra in figure S7 (see Supporting Information [S4]) further confirm that the olefinic moiety is vicinal to the C-Se bond and (II) is proposed to be the general core structure.



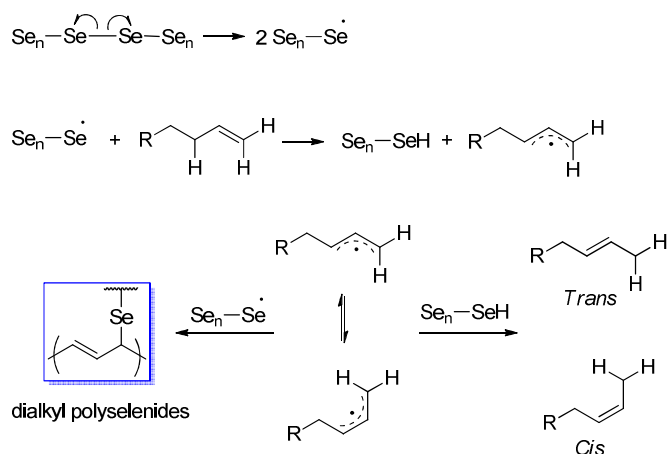
**Figure 3.**  $^1\text{H}$  and  $^{77}\text{Se}$  HMBC NMR analysis of Se containing species. As indicated in the image,  $^{77}\text{Se}$  NMR signals at  $\delta = 373.3$  and  $373.1$  ppm correlate with  $^1\text{H}$  multiplet  $\delta = 1.73$  and  $1.54$  ppm.

Mass values collected from ESI and MALDI MS analysis suggested the species **(III)** as plausible structures being formed. Detail mass spectra can be found in the supplementary information (S1 and S2). A correlation of NMR and mass spectrometry analysis results are listed in the Table S1.



### III

Based on the analysis of the NMR, FTIR, MS data in figures 1- 3 and table S1, the dissolution of Se in 1-ODE can be rationalized in terms of a radical process thermally initiated by the homolytic cleavage of Se-Se bond as highlighted in Scheme 1. The key step is the attack to the allylic proton in 1-ODE by Se radicals leading to the migration of the double bond and subsequent H transfer from the Se intermediate species.<sup>17, 21</sup> This is further supported by subsequent experiments where no isomerization is observed upon extensive heating of 1-ODE in the absence of Se (shown in figure 1b and also supporting information [S5]). Moreover, no dissolution of Se takes place under similar conditions if 1-ODE is replaced by octadecane, which lacks the alkene functionality.



**Scheme 1.** Proposed mechanism for the thermally induced Se radical attack to the allylic proton in 1-ODE, leading to the dissolution of Se and the migration of the terminal olefin. Highlighted in the blue frame is the olefinic group alpha to the C-Se bond which is a common feature present in the organoselenium species.

### 3.2 Dissolution of Se into oleylamine

In addition to 1-ODE, oleylamine is another solvent often used for the preparation of Se precursors.<sup>12a</sup> In our recent work, organoselenium species were detected by employing mass spectroscopy and <sup>1</sup>H and <sup>13</sup>C NMR, during the Se dissolution in oleylamine.<sup>22</sup> Although isomerization of the double bond was also identified in this instance, the depletion of olefin moiety was also observed, which did not occur in the case of 1-ODE.<sup>22</sup> Figure 4 shows the HSQC NMR analysis of Se containing species at steps (I) and (IV). A significant decrease in the signals at <sup>13</sup>C δ = 130 ppm and <sup>1</sup>H δ = 5.35 ppm upon heating at 200°C over prolonged periods of time (steps IV, highlighted in Figure 4b) is consistent with our previous reported results.<sup>22</sup> The disappearance of this signal occurs concomitantly with the dissolution of Se.

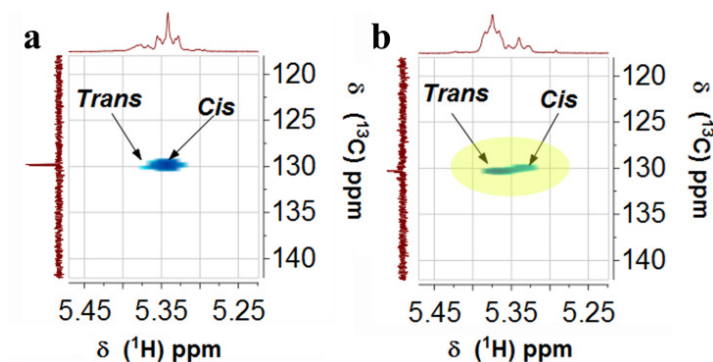


**Figure 4.** 2D HSQC NMR analysis of (a) Se and oleylamine mixture before heating; (b) Se and oleylamine after heating at 200 °C for 20h.

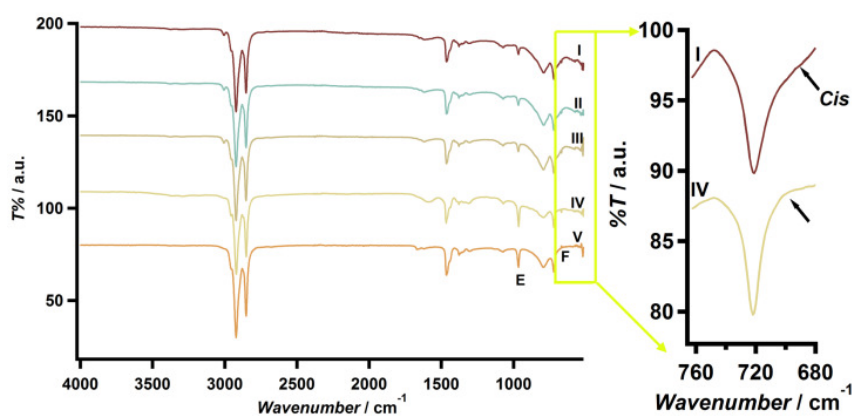


**Figure 5.** FTIR analysis the reaction of oleylamine with Se: (I) oleylamine mixed with Se before heating; (II) oleylamine and Se mixture after heating at 60°C under vacuum for 30min; (III) oleylamine and Se after heating at 130 °C under vacuum for 30min. (IV) oleylamine and Se after heating at 200 °C under Ar for 30min. (V) oleylamine and Se after heating at 200°C under Ar for 20h.

Figure 5 displayed FTIR spectra of Se containing species at steps (I) to (IV). The *cis* and *trans* isomerization is detected in the case of Se dissolution. As shown in Figure 5, *cis* hydrogen out of plane deformation (as highlighted, 'band F', step I) almost disappeared and an increasing of *trans* (band 'E') is observed after the total dissolution of Se (step IV). This observation is consistent with the HSQC NMR results shown in Figure 4 and our previous

report which further confirm the disappearance of the olefinic moiety during the Se dissolution in oleylamine.<sup>22</sup>

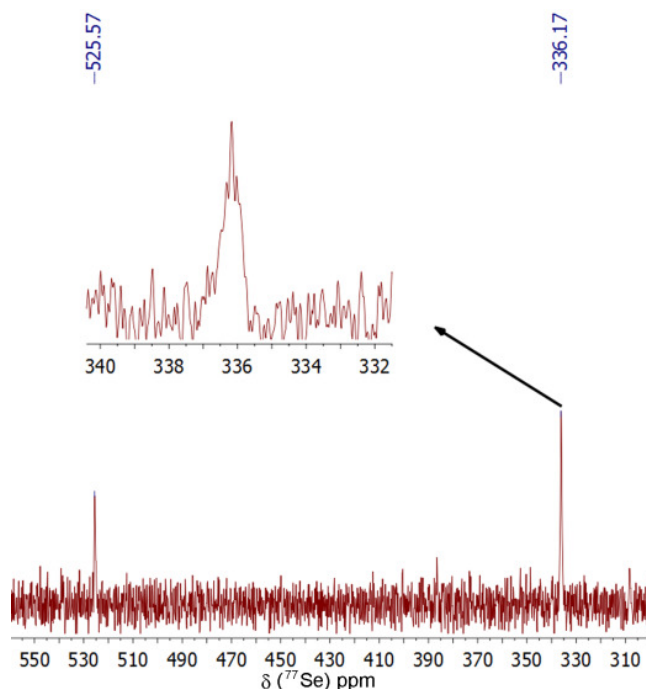


**Figure 6.** Proton decoupled  $^{77}\text{Se}$  NMR spectrum of the purified Se intermediate generated after dissolution in oleylamine after 20h at 200°C under Ar. Inset shows the enlarge image of the multiplet peak at  $\delta = 336.2$  ppm.

Figure 6 shows the  $^{77}\text{Se}$  NMR spectrum of the Se precursor generated at stage V. Two major signals at  $\delta = 336.2$  and 525.6 ppm show the characteristic peaks for polyalkyl polyselenides compounds.<sup>20</sup> This result is similar to our previous findings on Se dissolution into 1-ODE. Moreover,  $^{77}\text{Se}$  NMR shows the presence of a multiplet (highlighted in the inset image,  $\delta = 336.2$  ppm) indicating the formation polyalkyl polyselenides structure.

Figure 7 displays the 2D  $^1\text{H}$  and  $^{77}\text{Se}$  HMBC analysis of the Se precursor in oleylamine. The main  $^{77}\text{Se}$  signal  $\delta = 336.2$  ppm correlates to protons at chemical shifts of  $\delta = 2.81$ , 1.55 and 1.32 ppm. It should be noted that these results are comparable to those in Figure 3, except for the new signal at 2.81 ppm. Moreover, the  $^1\text{H}$  and  $^{13}\text{C}$  HMBC NMR spectrum in Figure S9a (see supporting information [S6]) suggest that the secondary carbon bound to Se is next to carbons with chemical shifts at  $\delta = 26.79$  and 47.24 ppm. The HSQC spectrum in Figure S9b shows these carbons are CH and  $\text{CH}_2$  moieties. The analysis also

shows that CH is attached to nitrogen ( $^1\text{H}$  at  $\delta=2.76$  and  $^{13}\text{C}$   $\delta=26.78$  ppm). Therefore, besides structure II, and polyalkyl polyselenides structures proposed previously,<sup>22</sup> structure IV is proposed to be one of the other core structures formed after consumption of the olefin moiety.

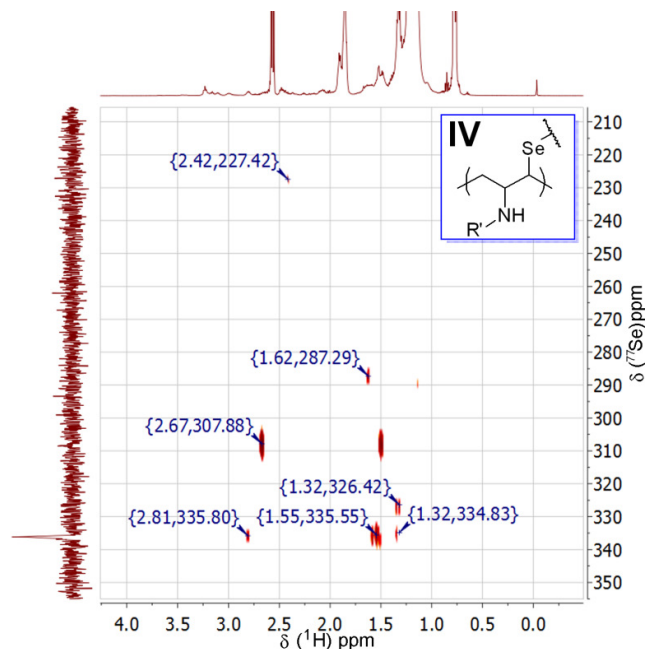
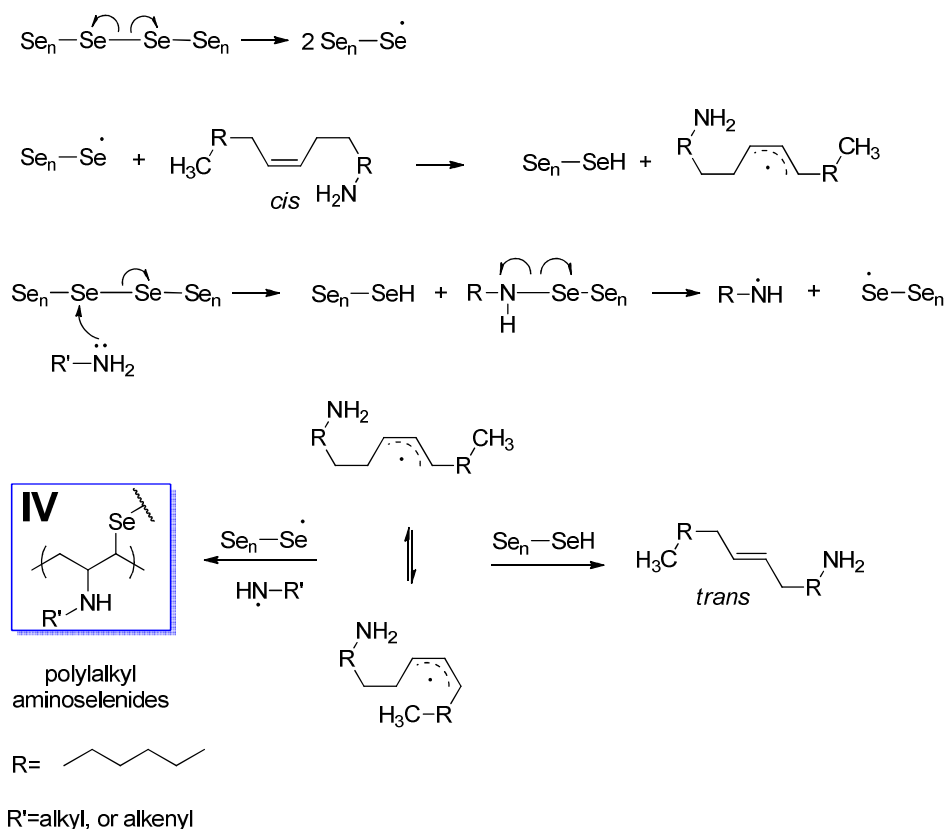


**Figure 7.**  $^1\text{H}$  and  $^{77}\text{Se}$  HMBC NMR spectra of the Se precursor in oleylamine. As indicated in the image,  $^{77}\text{Se}$  (multiplet,  $\delta = 336.17$  ppm) correlates with protons  $^1\text{H}$  (multiplet) at  $\delta = 2.81$ , 1.55 and 1.32 ppm.

The disappearance of the olefin group during Se dissolution in oleylamine can be explained by nucleophilic attack of oleylamine. Besides the double bond, oleylamine also possess a nucleophilic amine group capable of reacting with  $\text{Se}^{23}$  forming N-Se intermediates able to form N-centred radical species. Therefore, the organoselenium structures generated in the oleylamine approach are expected to be more complicated. Based on the NMR, FTIR analysis and previous results, a plausible reaction mechanism for the depletion of olefin moiety during Se dissolution in oleylamine is proposed in Scheme 2. A radical process is thermally initiated by the homolytic cleavage of the Se-Se bond as highlighted in Scheme 2. The key step is the attack on the *cis* allylic proton in oleylamine by Se radicals, leading to the isomerization of the double bond and subsequent H transfer from the Se intermediate species.<sup>21</sup> Concomitantly, nucleophilic addition from the amine occurs with subsequent addition to the alkyl chain as shown in the Scheme 2.



**Scheme 2.** Proposed mechanism for the thermal induced Se radical attack on oleylamine, leading to the dissolution of Se and the disappearance of the olefin group.

### 3.3. Se dissolution into 1-ODE promoted by AIBN

On the basis that Se solubilisation in 1-ODE occurs via radical species, we investigated whether trace amount of AIBN could accelerate this process. For instance, recent studies by Yu et al. have shown that radical cycloaddition reactions involving elemental chalcogens can be accelerated in the presence AIBN.<sup>24</sup> Figure 8 shows clear evidences of migration of the olefin group, and the associated Se dissolution, just after 1 h heating at 200°C in the presence of AIBN. Indeed, the <sup>13</sup>C NMR signals at  $\delta = 124.4$  and 131.7 ppm (figure 8a) as well as the <sup>1</sup>H NMR multiplet at  $\delta = 5.42$  ppm (figure 8b) can be observed after 1h as opposed to 20h in the absence of AIBN (figure 1). The migration of the double bond is further confirmed by HSQC NMR (figures 8c and 8d) as well as FTIR (figure 8e), suggesting that AIBN effectively promotes the dissolution of Se. AIBN decomposes at temperature above 65°C, eliminating molecular nitrogen and generating 2-cyanoprop-2-yl radicals acting as initiators.<sup>25</sup> It should be mentioned that, in the absence of Se, the migration of the olefin moiety is not observed when AIBN is present. Consequently, it could be concluded that the radical initiator

assists the generation of Se radicals which subsequently attack the  $\gamma$ -H in 1-ODE as suggested in Scheme 1.

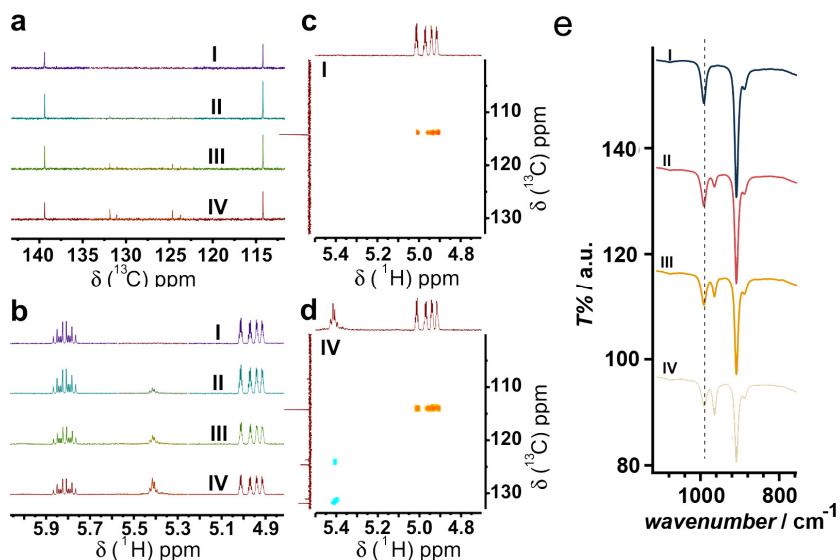


**Figure 8.**  $^{13}\text{C}$ -NMR (a) and  $^1\text{H}$ -NMR (b) analysis of Se/1-ODE mixture at room temperature (step I) and after loading AIBN and heating at  $200^\circ\text{C}$  for 1 (step II), 2 (step III) and 3h (step IV) under Ar. HSQC 2D NMR of the mixture at steps I (c) and IV (d). FTIR spectra of the solutions at the various stages (e). The main features of the various spectral responses are identical to those highlighted in figure 1, although AIBN containing solution promotes Se solubilisation within 1 h.

Reported times for Se dissolution in 1-ODE at various concentration and temperatures are summarised in table S2 (supporting information). The time required for solubilisation of  $0.1 \text{ mol}\times\text{dm}^{-3}$  significantly decreases from 48 hr at  $150^\circ\text{C}$  to between 1 or 2 hr at  $200^\circ\text{C}$ . Our measurements in the presence of 1 mg of AIBN show slightly shorter times for this Se concentration. The remarkable point is observed at concentrations in the range of  $1.0 \text{ mol}\times\text{dm}^{-3}$ , where the dissolution time is decreased from 20 to 3 hr in the presence of AIBN. This temperature is still below the melting point of Se ( $221^\circ\text{C}$ ).<sup>26</sup> Furthermore, the main by-products of AIBN decomposition are traces of short chains volatile alkanes which do not compromise the purity of the final material.

### 3.4 CdSe QDs synthesis employing Se precursors generated in the presence of AIBN

CdSe QDs showing high degree of monodispersity and strong absorption-luminescence overlap were obtained employing Se precursors in 1-ODE in the presence of AIBN as shown in figure 9. The TEM micrograph in figure 9a shows highly monodispersed  $3.0 \pm 0.2\text{nm}$  dots



obtained after 15 min growth time. The inset in figure 9a displays absorption and luminescence spectra featuring a strong spectral overlap and a progressive decrease of the optical band gap with increasing growth times.

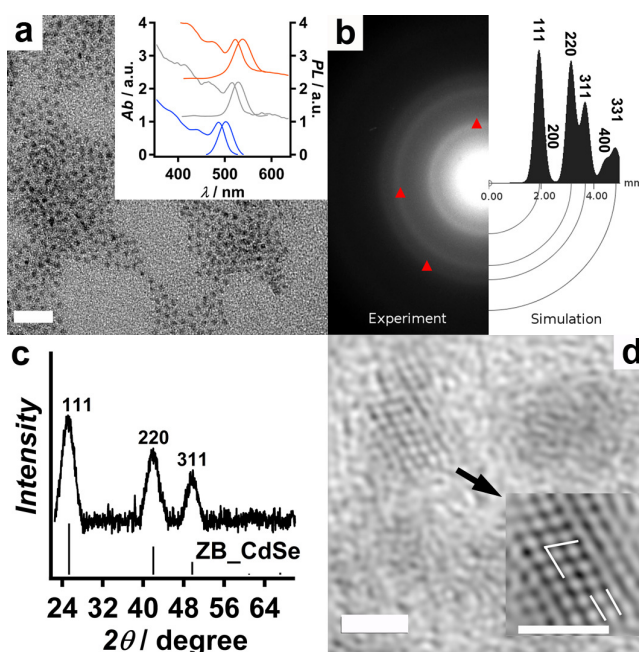


**Figure 9.** Characteristic TEM micrograph (scale bar 20 nm) of  $3.0 \pm 0.2$  nm CdSe dots after 15 min growth (a). The inset shows the absorption and luminescence spectra recorded after 3 (blue), 8 (grey) and 15 min (red) growth time. Experimental and simulated selected area electron diffraction patterns (b), powder XRD (c) and high resolution TEM image (d, scale bar 2nm) of CdSe dots. XRD pattern for cubic CdSe (PDF 19-0191) is also shown in (c). The inset in (d) shows a 3.0 nm dot, highlighting the  $70 \pm 2^\circ$  cross grating originating from adjoining (111) planes in fcc crystals with a lattice spacing of  $3.5 \pm 0.2 \text{ \AA}$  (parallel lines).

Selected area electron diffraction pattern rings in figure 9b are characteristic of zinc blende (ZB) unit cell, with the 111, 220 and 311 rings clearly identifiable although broadened by the nanoscopic dimension of the crystals. The experimental data correlates closely with simulations of the diffraction patterns for face-centered cubic 3 nm CdSe nanocrystals.<sup>27</sup> X-ray powder diffraction (figure 9c) is fully compatible with phase pure ZB CdSe dots. Figure 9d shows a typical high resolution TEM image obtained from as-prepared 3nm CdSe QDs, featuring a cross-grating pattern generated by adjoining (111) planes with  $70 \pm 2^\circ$  angle. The measured lattice spacing of the (111) plane of  $3.5 \pm 0.2 \text{ \AA}$  is close to the value expected for cubic CdSe (inset image of figure 9d).

These results show that the presence of traces amount of AIBN do not affect the nucleation of CdSe, demonstrating its suitability for the preparation of Se precursors for QD synthesis. The ability of preparing chalcogenide precursors with high concentration and short times are crucial for deployment of scalable routes for the production of thin-film photovoltaic devices. The introduction of radical initiators in phosphine-free solvents, along with temperature and concentration, provides an additional optimisation parameter that can be exploited in this direction.

## 4. Conclusions

Our studies have unveiled the processes taking place during the dissolution of Se in 1-ODE and oleylamine, an important bottleneck in the scale-up of phosphine-free synthesis of CdSe QDs. The process is initiated by the generation of Se radicals which attack the allylic proton in both solvents. This reaction manifests itself by the migration of the olefin group in 1-ODE and isomerization in oleylamine.

In the case of 1-ODE, the most plausible intermediates in this process are identified as 1,3-di(octadec-3-en-2-yl)monoselenide, 1,3-di(octadec-3-en-2-yl)diselenide and 1,3-di(octadec-3-en-2-yl)triselenide. On the other hand, the intrinsic nucleophilic properties of oleylamine facilitate the reaction with the double bond during the Se solubilisation, inducing the formation of polyalkyl aminoselenides besides the polyalkyl polyselenide species.

For the first time, we show that addition of trace amount of AIBN significantly accelerates the solubilisation of Se in 1-ODE in the molar concentration range. Studies carried out at various concentrations and temperatures indicate that Se solubilisation requires temperatures above 150°C, even in the presence of AIBN. Although AIBN promotes faster Se dissolution in the 0.1 mol×dm<sup>-3</sup> concentration range, the strongest effects are observed at significantly higher Se concentrations.

The utilisation of AIBN as a promoter in the generation of Se precursors allows the facile phosphine-free synthesis of high-quality zinc-blend CdSe QDs without the need of further additives. The crystal structure of the dots contrasts with the strong wurtzite character of the materials obtained in the presence of phosphine groups.<sup>28</sup> We strongly believe that optimization of the chalcogenide precursor's composition by adjusting the concentration of radical initiators, such as AIBN, can have a significant impact in scaling up the synthesis of these materials and their deployment in solution-processable photovoltaic technologies.

## Acknowledgement

The authors are grateful to Mr. Jonathan Jones, Mr Paul Lawrence and Dr. Craig Butts for their support to this research. This research is supported by the Engineering and Physical Sciences Research Council (EP/G031088/1, SUPERGEN Consortium on Excitonic Solar Cells (DJF and BH) and EP/J002542/1 (MCG and DBA)).

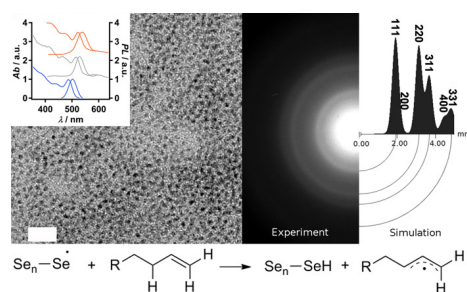
## Reference

1. Y. Shirasaki, G. J. Supran, M. G. Bawendi and V. Bulovic, *Nature Photonics*, 2013, **7**, 13-23.
2. (a) F. A. Esteve-Turrillas and A. Abad-Fuentes, *Biosensors & Bioelectronics*, 2013, **41**, 12-29; (b) F. Wang, X. Liu and I. Willner, *Adv. Mater.*, 2013, **25**, 349-377; (c) X. Michalet, F. F. Pinaud, L. A. Bentolila, J. M. Tsay, S. Doose, J. J. Li, G. Sundaresan, A. M. Wu, S. S. Gambhir and S. Weiss, *Science*, 2005, **307**, 538-544.
3. (a) L. Etgar, *Materials*, 2013, **6**, 445-459; (b) P. V. Kamat, *Journal of Physical Chemistry C*, 2008, **112**, 18737-18753.
4. (a) T. Trindade, P. O'Brien and N. L. Pickett, *Chem. Mater.*, 2001, **13**, 3843-3858; (b) C. B. Murray, D. J. Norris and M. G. Bawendi, *J. Am. Chem. Soc.*, 1993, **115**, 8706-8715.
5. (a) Z. A. Peng and X. Peng, *J. Am. Chem. Soc.*, 2000, **123**, 183-184; (b) L. Qu, Z. A. Peng and X. Peng, *Nano Lett.*, 2001, **1**, 333-337.
6. (a) C. de Mello Donegá, P. Liljeroth and D. Vanmaekelbergh, *Small*, 2005, **1**, 1152-1162; (b) K. L. Sowers, B. Swartz and T. D. Krauss, *Chem. Mater.*, 2013, **25**, 1351-1362.
7. B. Stewart, A. Harriman and L. J. Higham, *Organometallics*, 2011, **30**, 5338-5343.
8. J. Jasieniak, C. Bullen, J. van Embden and P. Mulvaney, *J. Phys. Chem. B*, 2005, **109**, 20665-20668.
9. (a) H. Shen, H. Wang, Z. Tang, J. Z. Niu, S. Lou, Z. Du and L. S. Li, *CrystEngComm*, 2009, **11**, 1733-1738; (b) M. Sun and X. Yang, *J. Phys. Chem. C*, 2009, **113**, 8701-

- 8709; (c) L. Liu, Z. Zhuang, T. Xie, Y.-G. Wang, J. Li, Q. Peng and Y. Li, *J. Am. Chem. Soc.*, 2009, **131**, 16423-16429.
10. S. Sapra, A. L. Rogach and J. Feldmann, *J. Mater. Chem.*, 2006, **16**, 3391-3395.
11. (a) Z. Deng, H. Yan and Y. Liu, *J. Am. Chem. Soc.*, 2009, **131**, 17744-17745; (b) B. Xing, W. Li, X. Wang, H. Dou, L. Wang, K. Sun, X. He, J. Han, H. Xiao, J. Miao and Y. Li, *J. Mater. Chem.*, 2010, **20**, 5664-5674.
12. (a) S. Mourdikoudis and L. M. Liz-Marzan, *Chem. Mater.*, 2013, **25**, 1465-1476; (b) Y. Wei, J. Yang, A. W. H. Lin and J. Y. Ying, *Chem. Mater.*, 2010, **22**, 5672-5677.
13. S. C. Riha, B. A. Parkinson and A. L. Prieto, *J. Am. Chem. Soc.*, 2011, **133**, 15272-15275.
14. Y. Liu, D. Yao, L. Shen, H. Zhang, X. Zhang and B. Yang, *J. Am. Chem. Soc.*, 2012, **134**, 7207-7210.
15. (a) S. Flamee, M. Cirillo, S. Abe, K. De Nolf, R. Gomes, T. Aubert and Z. Hens, *Chem. Mater.*, 2013, **25**, 2476-2483; (b) S. Flamee, R. Dierick, M. Cirillo, D. Van Genechten, T. Aubert and Z. Hens, *Dalton Trans.*, 2013, **42**, 12654-12661.
16. M. Ibanez, R. Zamani, A. LaLonde, D. Cadavid, W. Li, A. Shavel, J. Arbiol, J. R. Morante, S. Gorsse, G. J. Snyder and A. Cabot, *J. Am. Chem. Soc.*, 2012, **134**, 4060-4063.
17. (a) C. Bullen, J. van Embden, J. Jasieniak, J. E. Cosgriff, R. J. Mulder, E. Rizzardo, M. Gu and C. L. Raston, *Chem. Mater.*, 2010, **22**, 4135-4143; (b) R. García-Rodríguez, M. P. Hendricks, B. M. Cossairt, H. Liu and J. S. Owen, *Chem. Mater.*, 2013, **25**, 1233-1249.
18. W. W. Yu and X. Peng, *Angew. Chem. Int. Ed.*, 2002, **41**, 2368-2371.
19. J. D. Odom, W. H. Dawson and P. D. Ellis, *J. Am. Chem. Soc.*, 1979, **101**, 5815-5822.
20. H. Eggert, O. Nielsen and L. Henriksen, *J. Am. Chem. Soc.*, 1986, **108**, 1725-1730.
21. R. M. Hoyte and D. B. Denney, *J. Org. Chem.*, 1974, **39**, 2607-2612.
22. B. Hou, D. Benito-Alifonso, N. Kattan, D. Cherns, M. C. Galan and D. J. Fermín, *Chem. Eur. J.*, 2013, **19**, 15847-15851.
23. J. Lu, Y. Xie, F. Xu and L. Zhu, *J. Mater. Chem.*, 2002, **12**, 2755-2761.
24. L. Yu, Y. Wu, T. Chen, Y. Pan and Q. Xu, *Org. Lett.*, 2012, **15**, 144-147.
25. M. B. Smith and J. March, *March's Advanced Organic Chemistry: Reactions, Mechanisms, and Structure*, 6th edn., WILEY, 2007.
26. Y. A. Yang, H. Wu, K. R. Williams and Y. C. Cao, *Angew. Chem. Int. Ed.*, 2005, **44**, 6712-6715.
27. P. A. Stadelmann, *Ultramicroscopy*, 1987, **21**, 131-145.

28. (a) W. W. Yu, Y. A. Wang and X. Peng, *Chem. Mater.*, 2003, **15**, 4300-4308; (b) B. Hou, D. Parker, G. P. Kissling, J. A. Jones, D. Cherns and D. J. Fermín, *J. Phys. Chem. C*, 2013, **117**, 6814-6820; (c) Y. C. Li, H. Z. Zhong, R. Li, Y. Zhou, C. H. Yang and Y. F. Li, *Adv. Funct. Mater.*, 2006, **16**, 1705-1716.

## Table of content



Trace amounts of AIBN substantially accelerates the homolytic cleavage of Se-Se bond, facilitating the phosphine-free synthesis of CdSe quantum dots